PHYSICAL REVIEW D **94,** 116001 (2016)

Q-balls in DBI type *k* field theory

Masashi Kuniyasu,[*] Nobuyuki Sakai,[†] and Kiyoshi Shiraishi[‡]

Graduate School of Science and Engineering, Yamaguchi University, Yamaguchi 753-8512, Japan

(Received 20 September 2016; published 2 December 2016)

We of Q-balls in Dirac-Born-Infeld type k field theory, whose action includes a nonlinear kinetic term, $\sqrt{1-bg^{\mu\nu}\partial_\mu\phi^a\partial_\nu\phi^a}/b$. Specifically, for two potentials, $V_3 = m^2\phi^2/2 - \mu\phi^3 + \lambda\phi^4$ and $V_4 = m^2\phi^2/2 - \lambda\phi^4 + \phi^6/M^2$, we survey equilibrium solutions for the whole parameter space and analyze their stability through the use of catastrophe theory. Our analysis shows that V_3 and V_4 models fall into fold catastrophe and cusp catastrophe types, respectively, just as for canonical Q-balls. We also find that, as long as the absolute minimum of $V(\phi)$ is located at $\phi = 0$, equilibrium solutions exist without any additional constraint on charge Q no matter how large b (nonlinearity) is.

DOI: 10.1103/PhysRevD.94.116001

I. INTRODUCTION

Q-balls are the leading nontopological solitons in field theories. The original nontopological solitons were found by Freedberg *et al.* [1] in a model with a U(1) complex scalar field coupled to a real scalar field. Subsequently, Coleman found such solutions in a simpler model with an SO(2) [viz. U(1)] scalar field only, and called them Q-balls. [2]. In contrast to topological defects such as monopoles, these are stabilized by a Noether charge Q, and their energy is localized in a finite space.

It has been shown that Q-balls could form in the nonrenormalizable ϕ^6 potential model [3] or in the minimal supersymmetric standard model [4]. If Q-balls are formed efficiently by the Affleck-Dine mechanism [5], they could be responsible for baryon asymmetry [6] and the dark matter content of the Universe [7]. Moreover, the fate of neutron stars may be affected by Q-balls [8]. Thus, Q-balls may be important in particle physics, cosmology, and astronomy.

Based on those physical motivations, the stability of Q-balls has been intensively studied [9–11]. Paccetti Correia and Schmidt showed that the sign of $(\omega/Q)dQ/d\omega$ may play a role [10]. Later, Sakai and Sasaki discussed the stability through the use of catastrophe theory [11]. Their research was done not only on Q-balls but also Q-bubbles, which have absolute minima at $\phi \neq 0$, and they claimed that catastrophe theory is useful for analyzing the stability of Q-balls (and Q-bubbles) for the whole parameter space. They considered some potential models in their research.

Although previous work on Q-balls has been restricted to canonical scalar field theories, there is no reason that scalar fields in nature should be canonical. There may exist scalar fields with a nonlinear kinetic term, which are called k field theories. Here we focus on Dirac-Born-Infeld (DBI) theories because they are motivated by string theory [12] and many other phenomenological theories as discussed below.

The original DBI theory was suggested by Born and Infeld [13] for electromagnetic vector fields; however, their idea was subsequently extended to scalar or tensor field theories. Heisenberg introduced the DBI type k field theory to calculate hadron scattering in the fireball model [14]. Then, Dirac pointed out that the theory is an extensible electric models [15]. DBI type k field theories were also discussed in strong interaction physics [16] and topological defects [17]. In cosmology, k field theories were first introduced in the context of inflation [18] and then k-essence models were suggested as a solution to the cosmic coincidence problem [19].

It should be mentioned that nontopological solitons in k field theories were first studied by Diaz-Alonso and Rubiera-Garcia [20]; they established static soliton solutions, not Q-ball-like solutions with phase rotation.

In this article, we study Q-ball solutions in DBI type k field theory for two typical potentials. We also discuss stability by catastrophe theory, following Sakai and Sasaki [11].

We adopt the natural system of units, $c = \hbar = 1$, and the sign convention for metric $(+---)$.

II. BASIC EQUATIONS AND ANALYSIS METHOD

A. Field equation in DBI type *k* field theory

Let us consider an SO(2) symmetric k field, $\phi^a = (\phi^1, \phi^2)$, which is based on DBI theory. Its action is given by

$$\begin{aligned} S &= \int d^4x\mathcal{L}, \\ \mathcal{L} &\equiv -\frac{1}{b}\sqrt{1-2bX} + \frac{1}{b} - V(\phi), \\ \phi &\equiv \sqrt{\phi^a\phi^a} = \sqrt{(\phi^1)^2 + (\phi^2)^2}, \end{aligned} \tag{2.1}$$

[*]u003wa@yamaguchi-u.ac.jp
[†]nsakai@yamaguchi-u.ac.jp
[‡]shiraish@yamaguchi-u.ac.jp

where b is a constant which represents the nonlinearity of the field, and X is defined as

$$X \equiv \frac{1}{2} g^{\mu\nu} \partial_\mu \phi^a \partial_\nu \phi^a. \tag{2.2}$$

We assume that the field configuration is spherically symmetric and its phase rotates homogeneously,

$$(\phi_1, \phi_2) = \phi(r)(\cos \omega t, \sin \omega t). \tag{2.3}$$

The theory (2.1) has SO(2) symmetry; Noether's theorem tells us there is a conserved charge,

$$Q = \int d^3x \frac{\phi_1 \dot{\phi}_2 - \phi_2 \dot{\phi}_1}{\sqrt{1-2bX}} = \omega I,$$
$$I \equiv \int d^3x \frac{\phi^2}{\sqrt{1-2bX}}, \qquad \dot{} \equiv \frac{\partial}{\partial t}. \tag{2.4}$$

Canonical momentum is defined by

$$\Pi^a = \frac{\dot{\phi}^a}{\sqrt{1-2bX}}. \tag{2.5}$$

Then, the Hamiltonian of the system is given by

$$E = \int d^3x (\Pi^a \dot{\phi}^a - \mathcal{L})$$
$$= \frac{Q^2}{I} + \int d^3x \left\{ \frac{1}{b}\sqrt{1-2bX} - \frac{1}{b} + V(\phi) \right\}. \tag{2.6}$$

The variation of S with respect to ϕ under fixed ω, or equivalently, the variation of E with respect to ϕ under fixed Q, derives the field equation

$$\left(\frac{\phi'}{\sqrt{F}}\right)' + \frac{2}{r}\frac{\phi'}{\sqrt{F}} + \frac{\omega^2 \phi}{\sqrt{F}} = \frac{dV}{d\phi},$$
$$F \equiv 1 - b(\omega^2\phi^2 - \phi'^2), \qquad ' \equiv \frac{d}{dr}. \tag{2.7}$$

To solve the field equation (2.7) numerically, it is convenient to introduce an auxiliary variable, $\psi \equiv \phi'/\sqrt{F}$. Then Eq. (2.7) is rewritten as

$$\psi' = -\frac{2}{r}\psi - \frac{\omega^2\phi}{\sqrt{F}} + \frac{dV}{d\phi},$$
$$\phi' = \psi \sqrt{\frac{1-b\omega^2\phi^2}{1-b\psi^2}}. \tag{2.8}$$

B. Q-ball solutions

In preparation for studying Q-balls in DBI generalized SO(2) k field theory, we briefly review Q-ball solutions in the canonical scalar field ($b = 0$). The field equation (2.7) with $b \to 0$ reduces to

$$\phi'' = -\frac{2}{r}\phi' - \omega^2\phi + \frac{dV}{d\phi}. \tag{2.9}$$

This is equivalent to the field equation for a single static scalar field with the potential $V_\omega \equiv V - \omega^2\phi^2/2$. Q-ball solutions are supposed to be monotonically decreasing functions that satisfy boundary conditions

$$\phi'(0) = 0, \qquad \phi(\infty) = 0. \tag{2.10}$$

If one regards the radius r as "time" and the scalar amplitude $\phi(r)$ as "the position of a particle," one can understand Q-ball solutions in terms of Newtonian mechanics, as shown in Fig. 1. Equation (2.9) describes a one-dimensional motion of a particle under the conserved force due to the potential V_ω and the "time"dependent friction $-(2/r)\phi'$. If one chooses the "initial position" $\phi(0)$ appropriately, the static particle begins to roll down the potential slope, climbs up, and approaches the origin over infinite time.

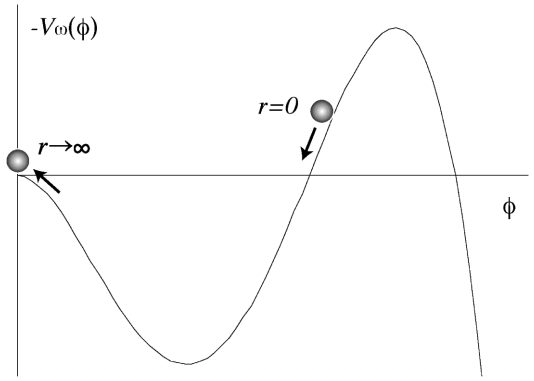

FIG. 1. Interpretation of Q-ball solutions in the canonical scalar field ($b = 0$) by analogy with a particle motion in Newtonian mechanics.

Figure 1 tells us the existence condition of solutions as follows. First, the initial position of the particle must be higher than the final position, which means $\min[V_\omega(\phi) > V_\omega(0) = 0$. Second, $-V_\omega(\phi)$ is convex upward about $r = 0$, which means $d^2V_\omega/d\phi^2(0) < 0$. These two conditions are summarized as

$$\omega^2_{\min} < \omega^2 < \omega^2_{\max},$$
$$\omega^2_{\min} = \min\left[\frac{2V}{\phi^2}\right], \qquad \omega^2_{\max} = m^2 \equiv \frac{d^2V}{d\phi^2}(0). \tag{2.11}$$

The two limits $\omega^2 \to \omega^2_{\min}$ and $\omega^2 \to \omega^2_{\max}$ correspond to the thin-wall limit and the thick-wall limit, respectively.

Now we consider the field equation (2.7) with the boundary conditions (2.10). Because the effective potential

V_ω cannot be well defined, we cannot apply the above argument by analogy with a particle motion to this general case. However, as long as Q-ball solutions exist, ϕ approaches zero as r goes to infinity. Accordingly, the field equation (2.7) asymptotically becomes

$$\phi'' \approx -\frac{2}{r}\phi' - \omega^2\phi + m^2\phi, \qquad (\phi \sim 0). \tag{2.12}$$

Therefore, the convex condition $d^2V_\omega/d\phi^2(0) < 0$ applies to this case and we obtain the same condition for $\omega_{\max}$,

$$\omega^2 < \omega_{\max}^2 = m^2. \tag{2.13}$$

Although it is difficult to discuss $\omega_{\min}^2$ analytically, we speculate that thin-wall solutions appear in the case $\omega^2 \approx \omega_{\min}^2$. In the thin-wall limit, the scalar amplitude should take the form

$$\phi(r) \sim \begin{cases} \phi_0, & (r > R) \\ 0, & (r < R) \end{cases}, \tag{2.14}$$

where ϕ_0 and R are constants. Then the field equation (2.7) becomes

$$\frac{\omega^2\phi_0}{1 - b\omega^2\phi_0^2} \approx \frac{dV}{d\phi}(\phi_0), \qquad (r \le R). \tag{2.15}$$

We notice that the effect of the nonlinear term $b\omega^2\phi^2$ is significant in the thin-wall case.

Moreover, there is one more constraint,

$$1 - b\omega^2\phi^2 > 0, \tag{2.16}$$

to obtain real-number solutions in Eq. (2.7). However, as we shall show later, the inequality (2.16) never violate in equilibrium solutions no matter how large b is for the following reason: as we increase b, $\phi(r)$ in equilibrium solutions decrease so that $b\omega^2\phi^2$ does not exceed 1.

C. Applying catastrophe theory

In this subsection, we review how we apply catastrophe theory to the system of Q-balls, following Sakai and Sasaki [11]. The important point is to appropriately choose *behavior variable(s), control parameter(s)*, and a *potential* in the present system. Here we italicize technical terms in catastrophe theory. For a given b, potential $V(\phi)$, and charge Q, we consider a one-parameter family of perturbed field configurations (virtual displacement) $\phi_\omega(r)$ near the equilibrium solution $\phi(r)$. The one-parameter family is chosen to satisfy $I[\phi_\omega] = Q/\omega$. Then the energy is regarded as a function of $I[\phi_\omega] = Q/\omega$: $E(\omega) \equiv E[\phi_\omega]$.

When ϕ_ω is an equilibrium solution, it satisfies $\delta E/\delta\phi_\omega = 0$; because $dE/d\omega = (\delta E/\delta\phi_\omega)d\phi_\omega/d\omega = 0$, we can regard ω as a behavior variable and E as a potential. On the other hand, because the charge Q and the model parameters [b and the parameters in $V(\phi)$] are given by hand, we can regard them as control parameters. Hereafter the model parameters are labeled by $P_i (i = 1, 2, \ldots)$. Then, we analyze the stability of Q-balls as follows.

(i) We solve the field equations (2.8) that satisfy the boundary conditions (2.10) for various values of ω and the model parameters P_i.
(ii) We calculate Q by Eq. (2.4) for each solution to find the *equilibrium space* $M = \{(\omega, P_i, Q)\}$. We denote the equation that determines M by $f(\omega, P_i, Q) = 0$.
(iii) We find folding points of M, where $\partial P_i/\partial\omega = 0$ and $\partial Q/\partial\omega = 0$, which correspond to the stability-change points $\Sigma = \{(\omega, P_i, Q) | \partial f/\partial\omega = 0, f = 0\}$. This correspondence is a great advantage in applying catastrophe theory.
(iv) We calculate the energy (2.6) for some solutions around Σ to find whether each solution is a local maximum or a local minimum. Around the stability-change points Σ, two solutions with different E share the same Q; in most cases the solution with smaller E is stable while the other solution is unstable. Thus, we find the stability about the whole M.

The stability of Q-balls in the canonical scalar field ($b = 0$) has been studied intensively and is accordingly understood very well. In this paper we focus on how b changes the stability structure.

D. Potential

As for the potential $V(\phi)$, we consider two typical models that allow Q-ball solutions. One is what we call the V_3 model,

$$V_3 = \frac{m^2}{2}\phi^2 - \mu\phi^3 + \lambda\phi^4, \tag{2.17}$$

where λ, μ, and m^2 are positive constants. Kusenko and Shaposhnikov showed that Q-balls in this model are stable even in the thick-wall limit [8]. For our numerical analysis, we rescale the quantities as

$$\tilde{r} = \frac{\mu}{\sqrt{\lambda}}r, \quad \tilde{\phi} = \frac{\lambda}{\mu}\phi, \quad \tilde{\omega} = \frac{\sqrt{\lambda}}{\mu}\omega, \quad \tilde{m} = \frac{\sqrt{\lambda}}{\mu}m,$$
$$\tilde{b} = \frac{\mu^4}{\lambda^3}b, \quad \tilde{Q} = \lambda Q, \quad \tilde{E} = \frac{\lambda^{3/2}}{\mu}E. \tag{2.18}$$

The other is what we call the V_4 model,

$$V_4 = \frac{m^2}{2}\phi^2 - \lambda\phi^4 + \frac{\phi^6}{M^2}, \tag{2.19}$$

where M^2, λ, and m^2 are positive constants. We rescale the quantities as

$$\tilde{r} = \lambda M r, \qquad \tilde{\phi} = \frac{\phi}{\sqrt{\lambda} M}, \qquad \tilde{\omega} = \frac{\omega}{\lambda M}, \qquad \tilde{m} = \frac{m}{\lambda M},$$
$$\tilde{b} = \lambda^3 M^4 b, \qquad \tilde{Q} = \lambda Q, \qquad \tilde{E} = \frac{E}{M}. \tag{2.20}$$

For both models, when $\tilde{m}^2 < 1/2$, the absolute minimum is located at $\phi \neq 0$ and, accordingly, true vacuum bubbles may appear. Therefore, in this case Q-balls are called Q-bubbles.

Hereafter we omit the tilde $\tilde{}$.

III. NUMERICAL RESULTS

A. Review of canonical Q-balls ($b = 0$)

For reference, we review the main results in [11] for canonical Q-balls ($b = 0$). Figures 2 and 3 show the structures of the equilibrium spaces $M = \{(\omega, m^2, Q)\}$ and their catastrophe map $\chi(M)$ to the control planes $C = \{(m^2, Q)\}$ for the V_3 and V_4 models, respectively. Only the results for $\omega > 0$ are presented; the sign transformation $\omega \to -\omega$ changes nothing but $Q \to -Q$. The dash-dotted lines in M denote stability-change points Σ.

Because the equilibrium space alone does not tell us which lines (solid or dashed) represent stable solutions, one should evaluate the energy E for several equilibrium solutions. When there are double or triple values of E for a given set of the control parameters (m^2, Q), by energetics the solution with the lowest value of E should be stable and the others should be unstable. In the following subsection we shall discuss this point again by showing the Q-E diagrams in Figs. 8 and 11.

According to the configurations of $\chi(\Sigma)$ in the control planes in Figs. 2 and 3, it was found that the V_3 model falls into fold catastrophe form while the V_4 model falls into cusp catastrophe form. In the control planes, the numbers of stable and unstable solutions for each (m^2, Q) are represented by No, S, U, SU, and SUU (see the figure captions for their definitions).

These figures let us understand the stability structures of the two models as follows. In the V_3 model:

(i) $m^2 \geq 1/2$: All equilibrium solutions are stable.

(ii) $m^2 < 1/2$ (Q-bubbles): For each m^2 there is a maximum charge, $Q_{\max}$, above which equilibrium solutions do not exist. For $Q < Q_{\max}$, stable and unstable solutions coexist. Stable Q-bubbles exist no matter how small Q is.

In the V_4 model:

(i) $m^2 \geq 1/2$: For each m^2 there is a minimum charge, $Q_{\min}$, below which equilibrium solutions do not exist. For $Q > Q_{\min}$, stable and unstable solutions coexist.

(ii) $m^2 < 1/2$ (Q-bubbles): For each m^2 there is a maximum charge, $Q_{\max}$, as well as a minimum charge, $Q_{\min}$, where stable solutions do not exist if $Q < Q_{\min}$ or $Q > Q_{\max}$. For $Q_{\min} < Q < Q_{\max}$, there are one stable and two unstable solutions. As m^2 becomes smaller, $Q_{\max}$ and $Q_{\min}$ come close to each other, and finally merge at $m^2 \approx 0.26$, below which there is no stable solution.

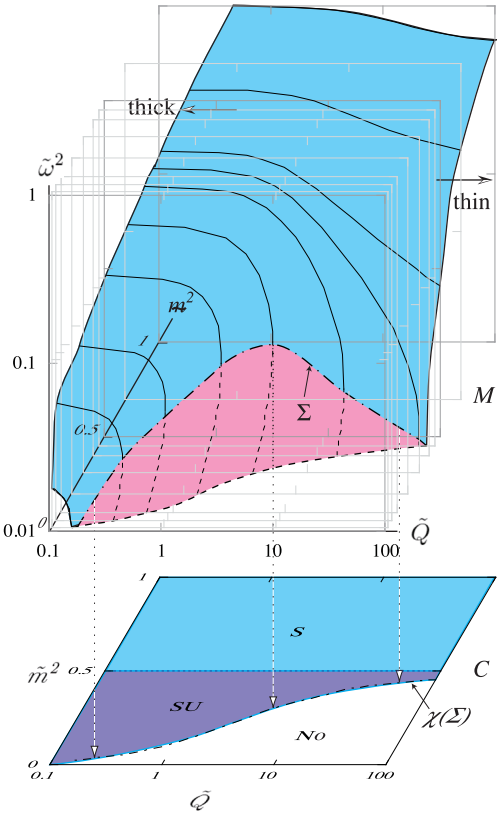

FIG. 2. Structures of the equilibrium space $M = \{(\omega, m^2, Q)\}$ and their catastrophe map $\chi(M)$ to the control plane $C = \{(m^2, Q)\}$ for the V_3 model. The dash-dotted lines in M denote stability-change points Σ, and the dash-dotted lines in C denote their catastrophe map $\chi(M)$. Solid lines in M (on the light-cyan-colored surface) and dashed lines (on the light-magenta-colored surface) represent stable and unstable solutions, respectively. The arrows indicated by "thin" and "thick" show the thin-wall limit, $\omega^2 \to \omega_{\min}^2$, and the thick-wall limit, $\omega^2 \to m^2$, respectively. In the regions denoted by S, SU, and No on C, there are the following solutions, respectively: one stable solution, one stable solution and one unstable solution, and no equilibrium solution, for fixed (m^2, Q). This figure is adapted from Ref. [11].

B. Q-balls in DBI type k field theory: V_3 model

Now we investigate Q-balls in DBI type k field theory, the field equation for which is given by Eq. (2.7) or Eq. (2.8). In this subsection we consider the V_3 model.

We show some profiles of $\phi(r)$ in Fig. 4. We fix $m^2 = 0.7$ and $\omega^2 = 0.36$, and see how the profile depends on b. Interestingly, though the amplitude with $b = 10$ is larger than that with $b = 0$, the amplitude becomes smaller as b increases further. To see the b dependence more clearly, we plot $\phi(0)$ as a function of b in Fig. 5. As b increases, $\phi(0)$

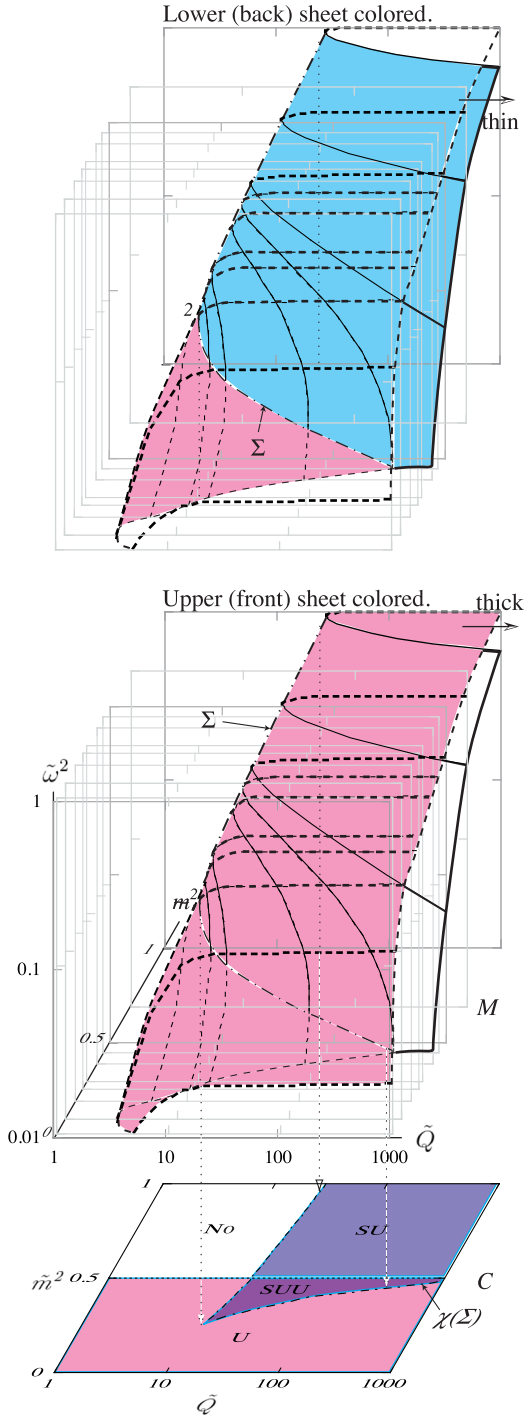

FIG. 3. The same as Fig. 2, but for the V_4 model. Because the structure of M is complicated in this case, we show two pictures of M. The upper panel shows the upper (front) sheet of the equilibrium space, while the middle figure shows the lower (back) sheet. In the regions denoted by No, U, SU, and SUU on C, there are the following solutions, respectively: no equilibrium solution, one unstable solution, one stable solution and one unstable solution, and one stable solution and two unstable solutions, for fixed (m^2, Q). This figure is adapted from Ref. [11].

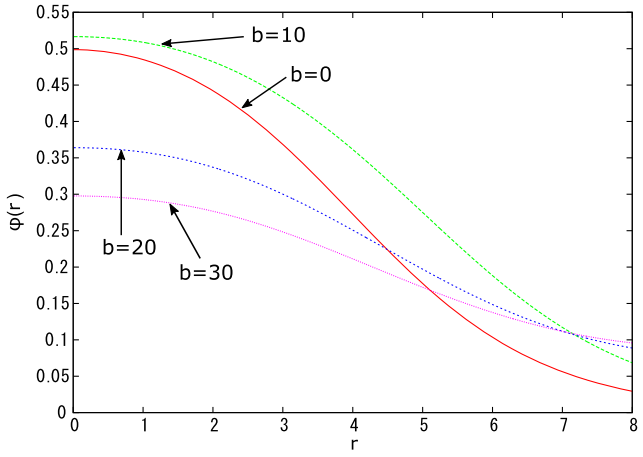

FIG. 4. Profiles of $\phi(r)$ for the V_3 model. We fix $m^2 = 0.7$ and $\omega^2 = 0.36$, and see how the profile depends on b.

temporarily increases until $b \sim 7$. However, as b goes to infinity, $\phi(0)$ approaches to zero. Because of this suppression mechanism, equilibrium solutions do not violate the condition (2.16) no matter how large b is.

Next, we discuss how the existence domain of the equilibrium solutions and their stability depends on b. Now the equilibrium space is $M = \{\omega, m^2, b, Q\}$ and the control space is $C = \{m^2, b, Q\}$. Because we cannot draw a 4D picture of M, we plot only its catastrophe map $\chi(M)$ to C in Fig. 6(a). Recall that $\chi(\Sigma)$ means the catastrophe map of the stability-change points Σ to C. To compare with the $b = 0$ case in Fig. 2, we show the cross section of $\chi(M)$ at several $b = \text{const}$ planes in Fig. 6(b). Furthermore, to see the effect of b on the solution structure clearly, we also show the cross section of C at $m^2 = 0.35$ in Fig. 7. These figures tell us the following:

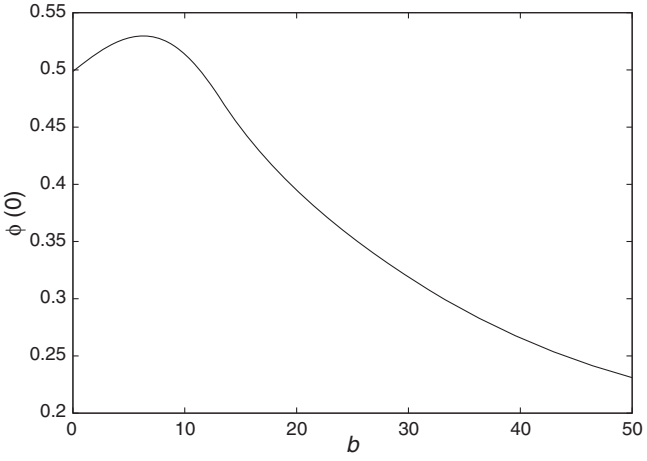

FIG. 5. $\phi(0)$ as a function of b for $m^2 = 0.7$ and $\omega^2 = 0.36$.

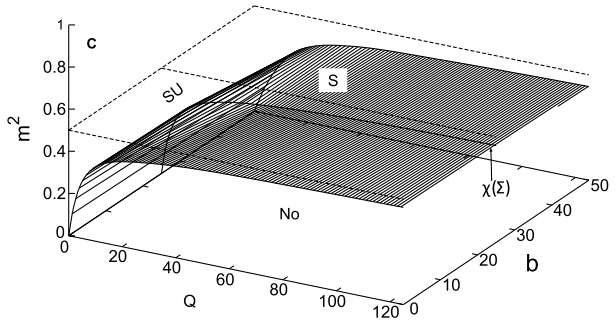

(a) *control space* $C = \{(m^2,\ b,\ Q)\}$

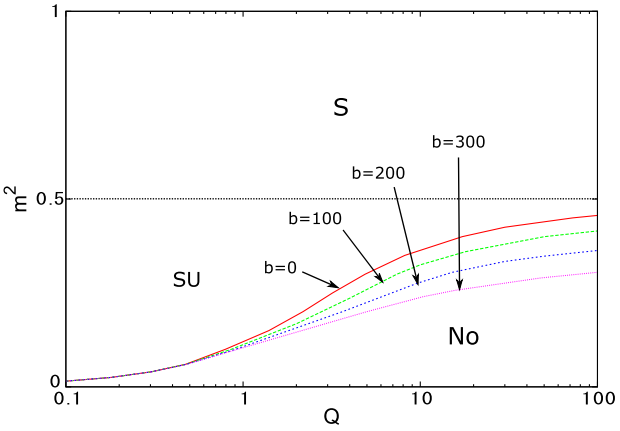

(b) *control planes* $C = \{(m^2,\ Q)\}$

FIG. 6. Catastrophe map $\chi(\Sigma)$ to the control space $C = \{(m^2, b, Q)\}$ for the V_3 model. The meanings of S, SU, and No are the same as in Fig. 2. (a) Three-dimensional diagram of $\chi(M)$ in C. (b) Cross sections of $\chi(M)$ at several $b = \text{const}$ planes. This shows how the Q-m^2 relation on $\chi(\Sigma)$ depends on b, as compared to Fig. 2.

(i) $m^2 \geq 1/2$: All equilibrium solutions are stable regardless of b.

(ii) $m^2 < 1/2$ (Q-bubbles): For fixed b and m^2 there is a maximum charge, $Q_{\max}$, above which equilibrium solutions do not exist. For $Q < Q_{\max}$, stable and unstable solutions coexist. As b increases for fixed m^2, $Q_{\max}$ also increases. This means that nonlinearity of DBI type k field extends the existence domain of (both stable and unstable) solutions.

(iii) The configuration of $\chi(\Sigma)$ indicates that the V_3 model falls into fold catastrophe. This means that the nonlinearity of the DBI type k field theory does not change the catastrophe type.

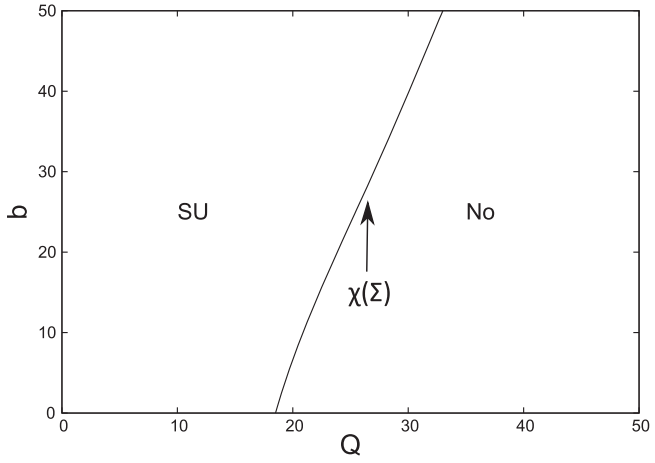

FIG. 7. Cross section of the control space in Fig. 6(a) at $m^2 = 0.35$. $\chi(\Sigma)$ means the catastrophe map to the $\{(b, Q)\}$ plane.

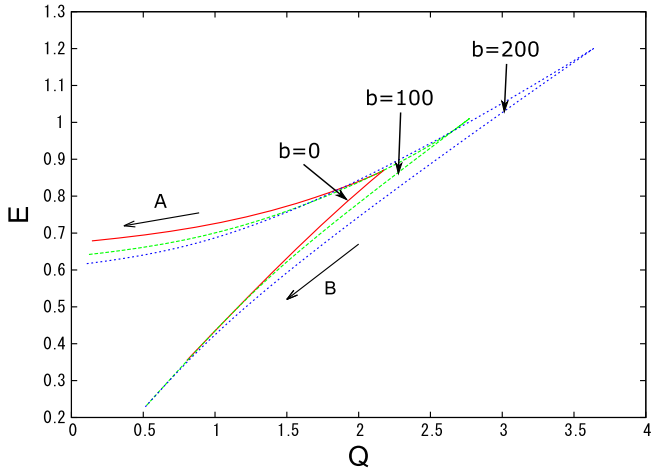

FIG. 8. Q-E diagram for V_3 Model with $m^2 = 0.2$. A and B denote the thin- and thick-wall limit, respectively.

Although we have already shown the stability of the equilibrium solutions by labeling them with S, U, etc., it is necessary to evaluate the energy E to understand the stability. Figure 8 is the Q-E diagram around a folding point on Σ. When there are double values of E for a given set of the control parameters (Q, b, m^2), by energetics the solution with the lowest value of E should be stable and the other should be unstable. We thus find the stability for the whole equilibrium space M.

C. Q-balls in DBI type k field theory: V_4 model

In the same way as for the V_3 model, we show the catastrophe map $\chi(M)$ to the control space $C = \{m^2, b, Q\}$ and its cross sections at several $b = \text{const}$ planes in Figs. 9(a) and 9(b), respectively. We also plot the cross section of C at $m^2 = 0.3$ in Fig. 10. These figures tell us the following.

(i) $m^2 \geq 1/2$: For fixed b and m^2 there is a minimum charge, $Q_{\min}$, below which equilibrium solutions do not exist. For $Q > Q_{\min}$, stable and unstable solutions coexist. As b increases for fixed m^2, $Q_{\min}$ also increases. This means that the nonlinearity of the DBI type k field theory shrinks the existence domain of (both stable and unstable) solutions.

(ii) $m^2 < 1/2$ (Q-bubbles): For fixed b and m^2 there is a maximum charge, $Q_{\max}$, as well as a minimum charge, $Q_{\min}$, where stable solutions do not exist if $Q < Q_{\min}$ or $Q > Q_{\max}$. For $Q_{\min} < Q < Q_{\max}$,

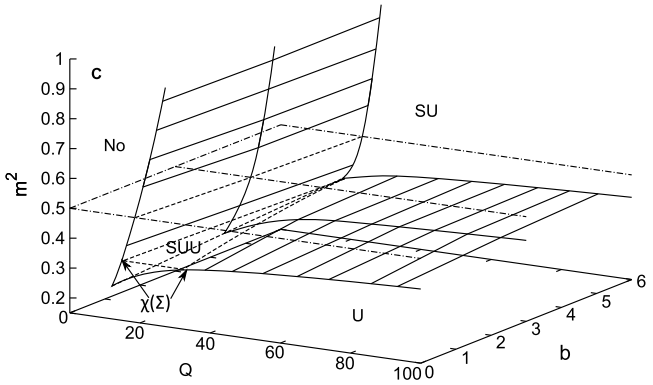

(a) *control space* $C = \{m^2,\ b,\ Q)\}$

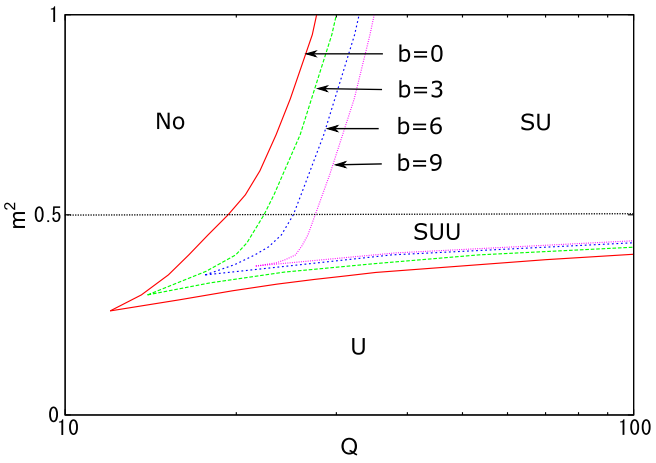

(b) *control planes* $C = \{(m^2,\ Q)\}$

FIG. 9. Catastrophe map $\chi(\Sigma)$ to the control space $C = \{m^2, b, Q\}$ for the V_4 model. The meanings of No, S, SU, and SUU are the same as in Fig. 3. (a) Three-dimensional diagram of $\chi(M)$ in C. (b) Cross sections of $\chi(M)$ at several $b =$ const planes. This shows how the Q-m^2 relation on $\chi(\Sigma)$ depends on b, as compared to Fig. 3.

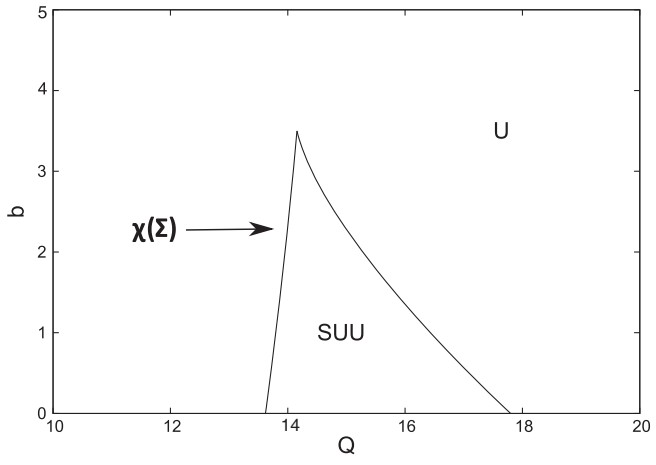

FIG. 10. Cross section of the control space in Fig. 9(b) at $m^2 = 0.3$. No stable solution exists when $b \gtrsim 3.5$. $\chi(\Sigma)$ means the catastrophe map to the $\{b, Q\}$ plane.

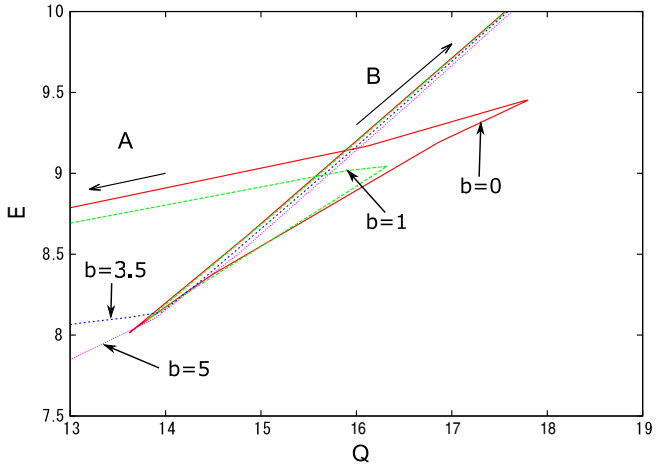

FIG. 11. Q-E diagram for the V_4 model with $m^2 = 0.3$. A and B correspond to the thin- and thick-wall limit, respectively.

there are one stable solution and two unstable solutions. As b increases for fixed m^2, $Q_{\max}$ and $Q_{\min}$ come close to each other and, finally, merge at one point, below which there is no stable solution. This means that the nonlinear effect of DBI type k field may kill Q-bubbles with large b and/or small m^2.

(iii) The configuration of $\chi(\Sigma)$ indicates that the V_4 model falls into cusp catastrophe, which is the same as in the canonical scalar field ($b = 0$).

Figure 11 is the Q-E diagram around a folding point on Σ. When there are triple values of E for a given set of the control parameters (Q, b, m^2), by energetics the solution with the lowest value of E should be stable and the others should be unstable. This figure lets us understand how the SUU region appears in the control space in Fig. 10 and how it shrinks as b increases.

IV. CONCLUSION AND DISCUSSIONS

We have studied nontopological solitons in DBI type k field theory and have found new solutions of Q-balls, which we call k-balls. For two potentials, (2.17) and (2.19), we have surveyed equilibrium solutions for the whole parameter space. Except for Q-bubbles, $\min[V(\phi)] < V(0) = 0$, equilibrium solutions exist without any additional constraint on charge Q no matter how large b (nonlinearity) is. The reason is that the amplitude of the scalar field $\phi(0)$ becomes larger as b becomes smaller so that the condition (2.16) is not violated.

We have also analyzed the stability of the Q-balls in DBI type k field theory through the use of catastrophe theory. Our analysis have shown that the V_3 and V_4 models fall into fold catastrophe and cusp catastrophe form, respectively, just as for the canonical Q-balls. In the V_3 model, as b increases, the existence domain of the solutions expands; that is, additional solutions are

generated by the nonlinear k term. In the V_4 model, on the other hand, it shrinks as b increases; that is, some solutions are killed by the nonlinearity. Our results as a whole suggest that catastrophe theory is a useful tool for noncanonical field theories.

Although we have investigated Q-ball solutions of DBI type k field theory in flat spacetime for only the two types of potential models, it may be interesting to extend our analysis to other phenomenological models or gravitating noncanonical Q-balls.

[1] R. Friedberg, T. D. Lee, and A. Sirlin, Phys. Rev. D **13**, 2739 (1976).

[2] S. Coleman, Nucl. Phys. **B262**, 263 (1985).

[3] M. S. Volkov and E. Wohnert, Phys. Rev. D **66**, 085003 (2002); B. Kleihaus, J. Kunz, and M. List, *ibid.***72**, 064002 (2005); B. Kleihaus, J. Kunz, and I. Schaffer, *ibid.***77**, 064025 (2008).

[4] H. P. Nilles, Phys. Rep. **110**, 1 (1984); A. Kusenko, Phys. Lett. B **405**, 108 (1997); *Nucl. Phys. B, Proc. Suppl.* 62A-C, 248 (1998).

[5] I. Affleck and M. Dine, Nucl. Phys. **B249**, 361 (1985).

[6] K. Enqvist and J. McDonald, Nucl. Phys. **B538**, 321 (1999); **B538**, 321 (1999); S. Kasuya and M. Kawasaki, Phys. Rev. D **62**, 023512 (2000).

[7] A. Kusenko and M. Shaposhnikov, Phys. Lett. B **418**, 46 (1998); I. M. Shoemaker and A. Kusenko, Phys. Rev. D **80**, 075021 (2009).

[8] A. Kusenko and M. Shaposhnikov, Phys. Lett. B **423**, 104 (1998).

[9] A. Kusenko, Phys. Lett. B **404**, 285 (1997); **406**, 26 (1997); T. Multamaki and I. Vilja, Nucl. Phys. **B574**, 130 (2000); M. I. Tsumagari, E. J. Copeland, and P. M. Saffin, Phys. Rev. D **78**, 065021 (2008).

[10] F. Paccetti Correia and M. G. Schmidt, Eur. Phys. J. C **21**, 181 (2001).

[11] N. Sakai and M. Sasaki, Prog. Theor. Phys. **119**, 929 (2008).

[12] K. G. Savvidy, Ph.D. thesis, Princeton University, 1999, arXiv:hep-th/9906075.

[13] M. Born and L. Infeld, *Proc. R. Soc. A* 144, 425 (1934).

[14] W. Heisenberg, Z. Phys. **133**, 79 (1952).

[15] P. A. M. Dirac, *Proc. R. Soc. A* 268, 57 (1962).

[16] T. H. R. Skyrme, *Proc. R. Soc. A* 260, 127 (1961); S. Deser, M. J. Duff, and C. J. Isham, Nucl. Phys. **B114**, 29 (1976); B. Dion, L. Marleau, and G. Simon, Phys. Rev. D **53**, 1542 (1996).

[17] E. Babichev, Phys. Rev. D **74**, 085004 (2006); **77**, 065021 (2008); S. Sarangi, J. High Energy Phys. 07 (2008) 018.

[18] C. Armendariz-Picon, T. Damour, and V. Mukhanov, Phys. Lett. B **458**, 209 (1999).

[19] C. Armendariz-Picon, V. Mukhanov, and P. J. Steinhardt, Phys. Rev. Lett. **85**, 4438 (2000); C. Armendariz-Picon, V. Mukhanov, and P. J. Steinhardt, Phys. Rev. D **63**, 103510 (2001); T. Chiba, T. Okabe, and M. Yamaguchi, Phys. Rev. D **62**, 023511 (2000); M. Malquarti, E. J. Copeland, and A. R. Liddle, Phys. Rev. D **68**, 023512 (2003); J. U. Kang, V. Vanchurin, and S. Winitzki, Phys. Rev. D **76**, 083511 (2007).

[20] J. Diaz-Alonso and D. Rubiera-Garcia, Ann. Phys. (Amsterdam) **324**, 827 (2009).